

Anion Channels

2413-Pos Board B383

Three Dimensional Reconstruction of CFTR Chloride Channel Using Single Particle Analysis

Kazuhiro Mio¹, Toshihiko Ogura^{2,1}, Muneyo Mio¹, Hiroyasu Shimizu³,

Tzyh-Chang Hwang⁴, Chikara Sato¹, Yoshiro Sohma^{5,4}.

¹National Institute of Advanced Industrial Science and Technology, Tsukuba, Japan, ²PRESTO, Japan Science and Technology Agency, Kawaguchi, Japan,

³Osaka Medical College, Takatsuki, Japan, ⁴University of Missouri,

Columbia, MO, USA, ⁵Keio University School of Medicine, Tokyo, Japan.

The cystic fibrosis transmembrane conductance regulator (CFTR) chloride channel is a membrane integral protein that belongs to an ATP-binding cassette superfamily. Mutations in the CFTR gene cause cystic fibrosis (CF) in which salt, water and protein transports are defective in various tissues. Here we have expressed wild-type human CFTR as a FLAG-fused protein in HEK293 cells heterologously, and purified it in three steps: anti-FLAG and wheat germ agglutinin affinity chromatographies and size exclusion chromatography. The stoichiometry of the protein was analyzed using various biochemical approaches, including chemical cross-linking, blue-native PAGE, size exclusion chromatography, and EM observation of antibody decorated CFTR. All these data support a dimeric assembly of CFTR. Using 5,039 automatically selected particles from negatively stained EM images, the 3D structure of CFTR was reconstructed at 2 nm resolution assuming a two-fold symmetry. CFTR presumably in a closed state is shown to be an ellipsoidal particle with dimensions of $120 \times 106 \times 162$ Å. It comprises a small dome-shaped extracellular and membrane-spanning domain, and a large cytoplasmic domain with orifices beneath the putative transmembrane domain. EM observation of CFTR/anti-R-domain antibody complex confirmed that two R-domains located around the bottom end of the larger oval cytoplasmic domain. This is the first clear 3D-structural presentation of CFTR molecule in 'tail to tail' dimeric configuration.

2414-Pos Board B384

A Triad of Residues F1296-N1303-R1358 in NBD2 of CFTR is Involved in ATP-driven Gating

Andras Szollosi¹, Paola Vergani², Laszlo Csanady¹.

¹Department of Medical Biochemistry, Semmelweis University, Budapest,

Hungary, ²Department of Neuroscience, Physiology and Pharmacology,

University College London, London, United Kingdom.

Despite the general agreement that dimerization of CFTR's two Nucleotide Binding Domains (NBDs) drives channel opening, little is known about how nucleotide binding to individual NBDs promotes dimer formation. We investigated the allosteric interaction between three NBD2 residues, F1296, N1303 and R1358, because statistical coupling analysis reveals coevolution of these positions. Considering frequently occurring pairs in the multiple sequence alignment, we chose mutations F1296S and N1303Q for building a mutant cycle. The mutations had no significant effect on the apparent ATP affinity measured in inside-out macropatches. However, we observed elevated ATP-independent activity ($P_{o,bas}$) in F1296S/N1303Q. $P_{o,bas}$ was 0.0048 ± 0.0024 , 0.0034 ± 0.0007 , 0.013 ± 0.0027 , and 0.115 ± 0.028 for WT, F1296S, N1303Q, and F1296S/N1303Q, respectively. A thermodynamic mutant cycle built on these values implies a change in coupling ($\Delta\Delta G = -5.74 \pm 1.45$ kJ/mol) between positions 1296 and 1303 upon channel opening in the absence of ATP. To study the coupling between these two positions in the presence of ATP, but under equilibrium conditions, we introduced the same mutations into a non-hydrolytic background (K1250R). The high ATP-independent basal activity caused by the F1296S/N1303Q double-mutation was preserved in non-hydrolytic background. In addition, the mean burst duration of F1296S/N1303Q/K1250R in saturating ATP - estimated from the monoexponential macroscopic current decay time course following ATP removal - was more than 3-fold longer (31.34 ± 4.99 s) than that of K1250R (8.25 ± 0.58 s), F1296S/K1250R (7.77 ± 0.48 s), or N1303Q/K1250R (9.09 ± 0.95 s), predicting a change in coupling ($\Delta\Delta G = -2.95 \pm 0.48$ kJ/mol) between positions 1296 and 1303 as the channel closes from the ATP-bound open conformation. Thus, the interaction between F1296 and N1303 is important to stabilize the open state but is not an important determinant of ATP affinity. The N1303-R1358 interaction is under current investigation.

2415-Pos Board B385

Using Correlation Analysis To Predict Pairs Of Energetically Coupled Residues At The NBD-TMD Interface In CFTR

Daniella Muallem, Arturo Araujo, Paola Vergani.

UCL, London, United Kingdom.

CFTR, whose failure causes cystic fibrosis, is a chloride channel, which belongs to the ATP binding cassette (ABC) transporter family. Like other

ABC proteins, CFTR consists of two halves, each containing a cytosolic nucleotide-binding domain (NBD1, NBD2) and a transmembrane spanning domain (TMD1, TMD2). ATP binding and hydrolysis at the NBDs control the CFTR gate, presumed to be in the TMDs. It remains unclear precisely how the NBD/TMD coupling is mediated.

We used correlation analysis to identify possible pairs of energetically coupled residues which might mediate direct interactions between the NBDs and the TMDs. First, since CFTR belongs to a subgroup of ABCs, which contain two very divergent NBDs, we constructed an alignment containing only similar, asymmetric transporters. We implemented 5 different correlation algorithms. The major difficulty with correlation analysis is the prevalence of false positives due to non-independence of sequences resulting from evolutionary constraints. Only one algorithm corrects for non-independence by referring to an inferred phylogenetic tree, resulting in a smaller output. The other 4 methods assume independence and assign a score to every possible pair of alignment positions. Only pairs scoring in the top 1% were included.

To select candidate pairs at the NBD/TMD interface we looked for pairs found with more than one algorithm and separated by less than ~15 Å on a Sav1866 based homology model of CFTR. We also checked the distributions of amino acids at the two positions on the inferred phylogenetic tree, to eliminate correlations clearly due to evolutionary branching. We identified several pairs which are close to sites which can be cross-linked after cysteine substitution. Functional characterization of the effects of mutations on single-channel kinetics is underway.

2416-Pos Board B386

Two Distinct Gating Cycles of CFTR Chloride Channels

MingFeng Tsai¹, Hiroyasu Shimizu², Yoshiro Soma³, Min Li¹,

Tzyh-Chang Hwang¹.

¹Missouri University, Columbia, MO, USA, ²Osaka Medical College, Osaka,

Japan, ³Keio University, Tokyo, Japan.

CFTR channels, at maximally effective [ATP], switch between open and closed states $1-2$ s⁻¹. Pyrophosphate (PPi), applied with ATP, slows down the gating cycle by locking the channel in a stable open state ($\tau_o \sim 30$ s). PPi alone, applied immediately following closing of ATP-opened channels, locks open the channel with the same open time constant. However, the open state induced by PPi long after ATP removal (> 2 min) assumes a lifetime of 1.5 s, indicating the presence of two different closed states with distinct responses to PPi. By altering the duration of ATP removal and measuring the response of closed channels to PPi, we estimated the lifetime of the closed state (C*) that enters the lock-open state to be ~30 s. Since the lifetime of the C* state can be modulated by N⁶-phenylethyl-ATP (P-ATP), a high-affinity ATP analog, or by mutations that lower the ATP binding affinity at NBD1, we propose that one ATP molecule remains tightly bound at NBD1 during this closed state. As the trapped ATP molecule should survive for numerous gating cycles before being replaced by a second ligand, we carried out single channel experiments where the perfusion solution containing 2 mM ATP ($r_{open} = 3.33 \pm 0.19$ s⁻¹; $\tau_{open} = 235 \pm 19.8$ ms) was directly (dead time ~40 ms) switched to one with 50 μM P-ATP. The P_o of the channel increases in two steps. The channel opening rate was immediately increased ($r_{open} = 4.88 \pm 0.45$ s⁻¹) upon solution exchange, while the open time was not prolonged until ~40s after the application of P-ATP ($\tau_{open} = 386.7 \pm 25.2$ ms). This result indicates two gating cycles; one is solely driven by fast ATP binding/hydrolysis in NBD2 while another involves slow dissociation of ATP in NBD1.

2417-Pos Board B387

CFTR: Differential Reactivity, State-dependent Accessibility And Blocker Occlusion Of Cysteines Substituted For Adjacent Residues In TM6

Yohei Norimatsu¹, Anthony Iveta², Christopher Alexander¹, Xuehong Liu¹,

Mark Sansom², David C. Dawson¹.

¹Oregon Health & Science University, Portland, OR, USA, ²University of

Oxford, Oxford, United Kingdom.

We and others have identified residues in transmembrane segment six (TM6) of the CFTR chloride channel where substituted cysteines react with externally applied, polar, thiol-directed probes. A scan of TM6 showed that the profile of reactivity differed for channel-permeant reagents, such as [Au(CN)₂]⁻, and channel-impermeant reagents, such as MTSET⁺ and MTSES⁻. A cysteine at 338 (T338C) reacted with both channel-impermeant and -permeant probes while a cysteine at 337 (F337C) was unreactive toward channel-impermeant probes but reacted with [Au(CN)₂]⁻. The reaction rate of [Au(CN)₂]⁻ was 200 times faster with T338C than with F337C. Furthermore, the reactivity of F337C was highly dependent on the activation state of the channel, being greatly reduced prior to channel activation. T338C exhibited much less pronounced dependence on the activation state. We also compared the ability of a presumed open-channel blocker, GlyH-101, to occlude reactions at the two cysteines. F337C was effectively protected from reaction toward [Au(CN)₂]⁻,

whereas the reactivity of T338C was much less sensitive to the presence of the blocker. Finally we used a homology model of CFTR to estimate the relative positions of 337 and 338 in relation to the anion-selective pore. The model predicts that, whereas 338 is positioned such that it would be expected to directly line the pore, 337 could be partially occluded by other helices. Further, a molecular dynamics simulation suggests that movement of the transmembrane helices would significantly alter occlusion of F337C and have much less effect on T338C. These results demonstrate that by combining a quantitative analysis of the reactivity of substituted cysteines with an atomic-scale CFTR model we can begin to reveal the architecture of the CFTR anion-selective pore. Supported by NIH, CF Foundation and American Lung Association.

2418-Pos Board B388

On the Mechanism of CFTR Inhibition by CFTRinh-172

Zoia Kopeikin, Min Li, Tzyh-Chang Hwang.
University of Missouri, Columbia, MO, USA.

CFTR is inhibited with high potency and selectivity by thiazolidinone, CFTRinh-172. It was reported that CFTRinh-172 decreased the P_o by increasing the mean closed time (τ_c) without changing the mean open time (τ_o). These findings lead to the conclusion that CFTRinh-172 acts on the closed state. However, our data show that CFTRinh-172 not only increases τ_c , but also decreases τ_o by ~40% ([CFTRinh-172] = 5 μ M). For wild type (WT)-CFTR, the dose response relationship of CFTRinh-172 shows a K_i of 1.433 ± 0.235 μ M. Interestingly, G551D-CFTR, which manifests a τ_c ~100 fold longer than that of WT-CFTR, demonstrates a similar degree of inhibition as WT-CFTR. In contrast, manipulating the channel open time dramatically affects the degree of inhibition. For example, 1 μ M CFTRinh-172 causes 49% inhibition of the ATP-induced current, but the same concentration of CFTRinh-172 inhibits 82% of the current elicited by N^6 -phenylethyl-ATP, a high affinity ATP analogue that opens CFTR with a longer open time. The K_i of CFTRinh-172 for WT-CFTR locked open by ATP and PPi was estimated to be 5-10 nM. This drastic shift of the dose-response relationship is also seen with E1371S CFTR, a hydrolysis-deficient mutant. Due to impaired hydrolysis at NBD2, the current relaxation of E1371S mutant upon ATP withdrawal is very slow, 0.012 ± 0.002 s^{-1} . In the presence of 5 μ M CFTRinh-172, the rate of current relaxation of E1371S increases to 0.289 ± 0.096 s^{-1} . This result indicates that the inhibitor acts after the channel is open. The rate of the recovery from inhibition is 0.0227 ± 0.0038 s^{-1} for WT-CFTR, but 0.0036 ± 0.0020 s^{-1} for WT-CFTR locked open by PPi, and 0.0022 ± 0.0004 s^{-1} for E1371S. We conclude that the open state of the channel is favorable for CFTRinh-172 action and that the longer the open state, the higher the affinity for CFTRinh-172.

2419-Pos Board B389

Functional Study of CBS Domain Interaction during Common Gating of CLC-0 Chloride Channel

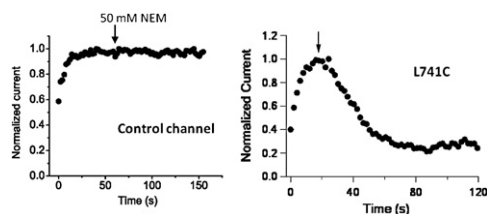
Ping Liang¹, Ekaterina A. Bykova¹, KeWei Wang², Jie Zheng¹.

¹UC Davis, Davis, CA, USA, ²Peking University School of Medicine, Beijing, China.

A pair of tightly interacting cystathionine β -synthetase (CBS) domains serves important regulatory functions in various protein families. Two CBS domains (CBS1 and CBS2) exist in the C-terminal of all CLC channels and appear to mediate most of the cytoplasmic inter-subunit interactions. Previous study in our lab indicates that common gating of CLC-0 is associated with a large conformational change in the C-terminal. How interaction between CBS domains affects common gating remains elusive.

Based on three recently reported crystal structures of the C-terminal of CLC channels (CLC-0, CLC-5 and CLC-Ka), we identified a set of residues that likely contribute to CBS interaction. Mutations at most of these positions affected the gating kinetics as well as the equilibrium of common gating. Preliminary data indicate that cysteine mutations at these positions can be modified by thiol-reactive reagents. Furthermore, the kinetics of common gating changed after cysteine modification. These results indicate that CBS domains do play an important role in common gating.

The figure shows the time course of NEM modification of L741C (right); the mutation was made in the control channel (left) background that lacked native reactive cysteines.



2420-Pos Board B390

Deuterium Isotope Effects On Fast Gating Of The Chloride Channel Clc-0

Giovanni Zifarelli, Michael Pusch.

Istituto di Biofisica, Genoa, Italy.

Gating of the *Torpedo* Cl⁻ channel CLC-0 is modulated by intracellular and extracellular pH, but the mechanism responsible for this regulation has remained so far elusive. Using inside-out patch clamp measurements we studied the dependence of the fast gate on pH_{int} and $[Cl^-]_{int}$. Only the closing rate, but not the opening rate showed a strong dependence on these intracellular factors. Using mutagenesis we excluded several candidate residues as mediators of the pH_{int} dependence. We propose a model in which a proton generated by the dissociation of an intrapore water molecule protonates E166 leading to channel opening. Deuterium isotope effects confirm that proton transfer is rate limiting for gate opening and that channel closure depends mostly on $[OH^-]$. The model is in natural agreement with the finding that only the closing rate constant, but not the opening rate constant, depends on pH_{int} and $[Cl^-]_{int}$.

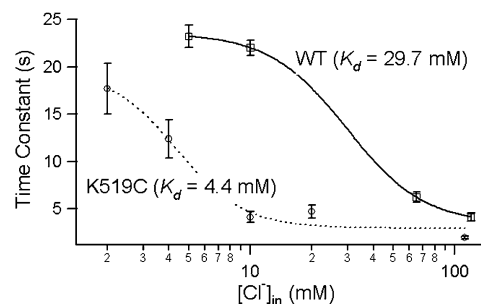
2421-Pos Board B391

R-helix Movement during Common Gating Affects Cl Binding in the CLC-0 Channel Pore

Ekaterina A. Bykova, Jie Zheng.

UC Davis, Davis, CA, USA.

Common (slow) gating of CLC-0 generates long silent periods in single-channel recordings and contributes significantly to regulation of Cl⁻ permeation. Our previous study suggests that movement of the pore-forming R-helix is directly coupled to common gating. We now report that R-helix movement appears to directly interfere with Cl⁻ binding in the pore. Binding of Cl⁻ to the pore facilitates common gate opening, while removing Cl⁻ slows down common gate opening. Mutations in R-helix that strongly affect common gating also appreciably shift the Cl⁻ dependence of channel open rate, apparently by altering the binding affinity of Cl⁻ in the pore. In this way, the common gating mechanism of CLC-0 is reminiscent of the fast gating, which also involves the control of chloride binding to the pore.



2422-Pos Board B392

Skeletal Muscle Chloride Channel, a Biophysical Sensor of Dystrophic Progression in Mdx Mouse, is a Potential Target of Pro-inflammatory Mediators

Anna Cozzoli, Sabata Pierno, Diana Conte Camerino, Annamaria De Luca.

Unit of Pharmacology, Faculty of Pharmacy, University of Bari, Bari, Italy.

A decrease in resting chloride channel conductance (gCl) characterizes myofibers of dystrophic mdx mouse in relation to both spontaneous degeneration, as in diaphragm, or exercise-induced damage as in fast-twitch EDL muscle (De Luca et al., *J. Pharmacol. Exp. Ther.* 2003). The molecular mechanism underlying gCl impairment might involve change in CLC-1 channel expression/turnover and/or function. Considering the role of inflammation in dystrophic damage, we tested if pro-inflammatory mediators may have CLC-1 channel as a target, through phosphorylating/dephosphorylating pathways. Two microelectrodes current clamp recordings were used to measure resting gCl in EDL and diaphragm muscle fibers from adult wild-type (wt) and mdx mice. In line with previous evidences, the *in vitro* application of phorbol dibutyrate (50 μ M) reduced gCl of wt EDL myofibers from 2610 ± 240 μ S/cm² (n=30) to 1265 ± 180 μ S/cm² (n=15). The application of TNF-alpha (1-30 ng/ml), a cytokine highly expressed in dystrophic muscle, to wt EDL fibers reduced gCl in a concentration-dependent manner with a maximal significant 20% decrease at 10-30 ng/ml. Angiotensin-II (10-100 nM), possibly involved in muscle degeneration and oxidative stress, produced a concentration-dependent decrease of gCl in wt EDL myofibers, with a 40 % decrease at 100 nM. The PKC-inhibitor chelerythrine (1 μ M) contrasted the effect of either phorbol ester, TNF-alpha or angiotensin-II. The application of 3.3 nM IGF-1 to diaphragm and EDL muscle fibers from exercised mdx mice, significantly counteracted the 40% impairment of gCl. Okadaic acid (0.25 μ M) fully prevented